# Potentialities of the digital holography in the study of the Fraunhofer diffraction pattern of microscopic objects

Journal of Physics: Conference Series **274** (2011) 012067 doi:10.1088/1742-6596/274/1/012067

# Potentialities of the digital holography in the study of the Fraunhofer diffraction pattern of microscopic objects

**J O Ricardo[1], M Muramatsu[2], F Palacios[1*], M Gesualdi[3], O Font[4], J L Valin[5], M Escobedo[6], S Herold[6], D F Palacios[7] and G F Palacios[1]**

[1] Department of Physics, University of Oriente, Cuba
[2] Department of General Physics, University of São Paulo - São Paulo, Brazil
[3] Engineering center, Models and Applied Social Science, UFABC - São Paulo, Brazil,
[4] Department of Bio-ingeniering, University of Oriente – Santiago de Cuba
[5] Mechanics Department, ISPJAE, Habana, Cuba
[6] Department of Computation, University of Oriente, Cuba.
[7] Department of Nuclear physics, University of Simón Bolíva, Venezuela

*Corresponding author's e-mail address: frpalaciosf@gmail.com

**Abstract**. A new method for microscopic object analysis is suggested in this research. We consider the diffraction theory combined with the image formation process, this combination constitutes the groundwork of many optic transformation processes that it has made possible to establish several modern applications of the Fourier optics processing and Digital Holographic Microscopy (DHM). Based on these optical applications we consider to study microscopic objects with regular forms starting from its Fraunhofer diffraction pattern obtained with DHM. The first results correspond to objects with regular forms and randomly distributed in the space, the second result corresponds to objects with regular forms and periodically distributed in the space. The objects' parameters can be determined with the diffraction pattern manipulation in a simple and accurate way. The biological and materials sciences can be beneficed with this research.

## 1. Introduction

The diffraction theory combined with the image formation process constitutes the groundwork of many optic transformation processes that it has made possible to establish several modern applications of the Fourier optics processing [1] and Digital Holographic (DH) [2, 3].

Most investigations about periodic apertures in the literature [4] deal with far-field diffraction and the analyses of circular apertures in a rectangular array presented in general to analyze the image shape in each small aperture with perpendicular incidence of light onto every pinhole in the array. Spectral analysis of three-dimensional images of microstructures is a powerful tool for materials science [5]. The determination of particle size distributions in the 1-200 μm size range is made using the principles of Fraunhofer Diffraction Pattern Analysis (FDPA). The technique [6] was first introduced by Swithenbank et al., in 1977. In FDPA, a laser beam is collimated to a diameter of a few millimeters and passed through a sample. The size distributions [7] of particles are important in many areas of science and engineering as in aerosol science, atmosphere and ocean sciences, chemical

engineering, combustion research and environment protection [8–12]. For particles that are significantly greater than the wavelength and with refractive indices that are substantially different from the unity, the dominant contribution to the near-forward scattered light can be accurately modeled by Fraunhofer diffraction theory. This approximation is valid for particles of radius greater than 2, 5 μm when analyzed with visible light ($\lambda \approx 500$nm) [13,14]. Although the rigorous Lorenz–Mie scattering theory is required in general cases [15], the validity of the diffraction approximation led to many applications.

Small angle light scattering had been applied for ellipsoidal red blood cells, commonly approximated by Fraunhofer diffraction [16] but calculus results show that better approximation from exact Mie theory is obtained by application of Anomalous diffraction, the derived expression show that the ellípticity of intensity curves in forward scattered light are equal to the ellipticíty of the red blood cell.

Digital holography (DH) has several features that make it an interesting alternative to conventional optical microscopy. These features include; an improved focal depth, possibility to generate three-dimensional images and phase contrast images [17,18]. The technique of DH has been implemented in a configuration of an optic microscope. The objective lens produces a magnified image of the object and the interference between this image and the reference beam is achieved by the integration of the microscope to one of the arms of a Mach-Zender interferometer. This configuration is called Digital Holographic Microscopy (DHM).

Interesting applications of DHM rely on the possibility of carrying out whole reconstruction of the recorded wave front and consequently, the determination of the phase and intensity distribution at any arbitrary plane located between the object and the recording plane, and along the object reconstructed image. Kreis and Jüpner [19] were the first to propose the application of digital holography to study the three-dimensional form of objects. Grilli et al. [20] used the DH possibility of reconstructing the image field at different planes from the object to find the object beam phase form to show how the experimental setup affects this. A method for 3D image reconstruction of transparent microscopic objects, based on the capture of only one off-axis hologram and the reconstruction field at different locations along the propagation direction, have also been proven [21]. Based on this possibility of the DH, in this study it is demonstrated that DHM provides valuable information about microscopic objects that they make possible quantitative extraction of lineal dimensions parameters from their diffraction pattern.

## 2. Experimental setup

Figure 1 shows the experimental setup used in this work, it correspond to a Digital Holographic Microscope designed for transmission imaging with transparent sample.

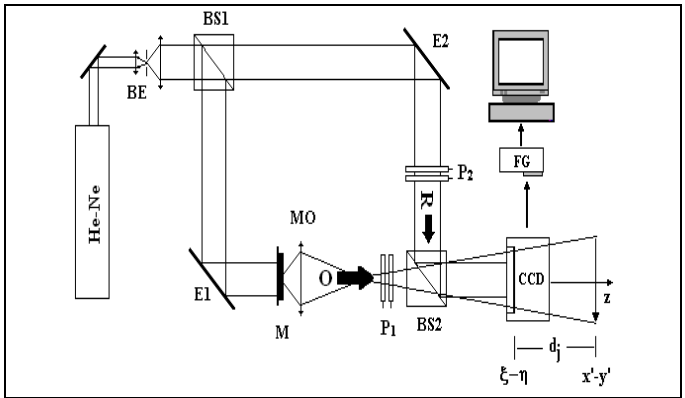


Figure 1. Experimental setup

A linearly polarized He-Ne laser (15 m W) is used as light source. The expanded beam from the laser is divided by the beam splitter (BS1) into reference and object arms. The microscope produces a magnified image of the object and the hologram plane is located between the microscope objective MO and the image plane (x'-y') at a distance $d_j$ from the recording hologram plane ($\xi$-$\eta$). In digital holographic microscopy we can consider the object wave emerging from the magnified image and not from the object itself [22].

The specimen M is illuminated by a plane wave and a microscope objective, that produces a wave front called object wave ***O***, collects the transmitted light. At the exit of the interferometer, the interference between the object wave ***O*** and the reference wave ***R*** creates the hologram intensity $I_H(\xi,\eta)$. A digital hologram is recorded by a CCD camera HDCE-10 with 4.65 µm of pixel size. The digital hologram $I_H(j,l)$ is an array of $M \times N$ = 768 x 768 8-bit-encoded numbers that results from the two-dimensional sampling of $I_H(j,l)$ by the CCD camera. For the image reconstruction is used the D*ouble* P*ropagation* M*ethod* (DPM) [23].

## 3. Methodology

In Digital Holographic Microscopy the field produced by the objective lens can be reconstructed along its propagation [24], figure 2a.

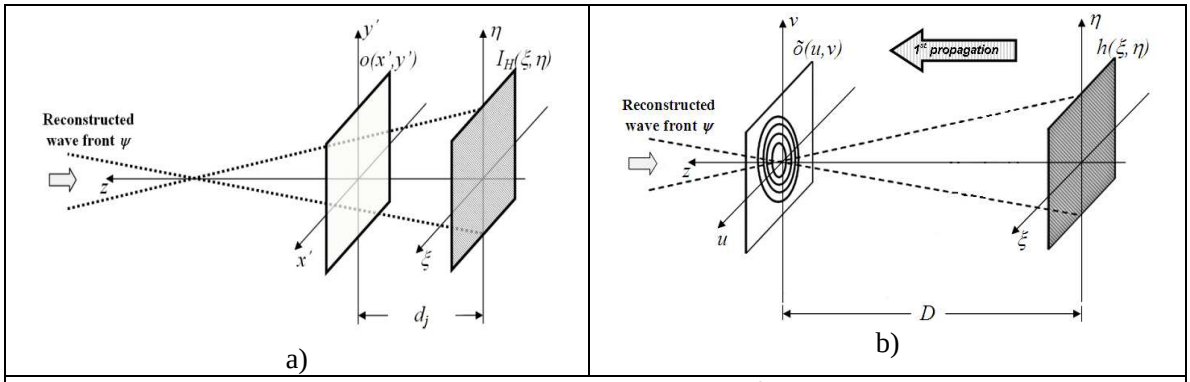


Figure 2. a) Image reconstruction in DHM, b) Reconstruction of the wave distribution $\tilde{o}(u,v)$ on the *(u-v)* plane.

The reconstruction of the complex wave distribution $\tilde{o}(u,v)$ on the *(u-v)* plane at reconstruction distance z = *D*, figure 2b, can be accomplish by means of the S*ingle* F*ourier* T*ransform* F*ormulation* (SFTF) [19]. The filtered complex wavefield in the same region defined by real image can be expressed by Eq. 1 by replacing the specimen hologram with a filtered hologram containing only spatial components of the real image [25],

$$\psi^{f}_{SFTF}(x',y',z=D)=A\exp\left[\frac{i\pi}{\lambda D}\left(x'^{2}+y'^{2}\right)\right]\Im\left\{I^{f}_{H}(\xi,\eta)\exp\left[\frac{i\pi}{\lambda D}\left(\xi^{2}+\eta^{2}\right)\right]\right\}_{[k_u,k_v]} \quad (1)$$

The complex field $\psi^{f}_{SFTF}$ is equivalent to the complex field distribution $\tilde{o}(u,v)$ on the back focal plane of the objective lens. From the Abbe's theory of image formation [26], the field on the back focal plane is related with Fourier Transform of the objects. It can be noted that calculating the intensity distribution from Eq. 1, the object's Fraunhofer diffraction pattern is obtained,

$$I_{SFTF}(x',y',z=D)=\left|\psi^{f}_{SFTF}(x',y',z=D)\right|^{2} \quad (2)$$

The Eq. (2) offers a powerful tool in micro objects analysis because with this, the manipulation of the Fourier plane can to be achieved and different techniques of Fourier optics can be apply digitally, such as pattern recognition, image processing and others.

Starting from the complex field described by Eq. (1), the complex wavefield $\psi(x',y',z=D,d')$ at an arbitrary $d'$ can be obtained by propagation of the wavefield $\psi^{f}_{SFTF}$ at the translational distance $d'$ and the result is inverse Fourier transformed,

$$\psi(x',y',z=D,d') = \Im^{-1}\left\{\psi^{f}_{SFTF}(x',y',z=D)\exp\left(i\,d'\sqrt{k^2+k_u^2+k_v^2}\right)\right\} \tag{3}$$

where $\Im^{-1}$ denotes the inverse Fourier transform, $k=2\pi/\lambda$, $k_u$ and $k_v$ the spatial frequencies corresponding to $u$ and $v$ respectively.

From Eq. 3 we can obtain the amplitude image $I(x',y',d'=d_j)$ by calculating the intensity,

$$I(x',y',d'=d_j) = \mathrm{Re}\left[\psi(x',y',z=D,d'=d_j)\right]^2 + \mathrm{Im}\left[\psi(x',y',z=D,d'=d_j)\right]^2 \tag{4}$$

and the phase image $\phi(x',y',d'=d_j)$ by calculating the argument,

$$\phi(x',y',d'=d_j) = arc\tan\left\{\frac{\mathrm{Im}\left[\psi(x',y',z=D,d'=d_j)\right]}{\mathrm{Re}\left[\psi(x',y',z=D,d'=d_j)\right]}\right\} \tag{5}$$

## 4. System magnification

In DHM the total system magnification depends on where it is placed the camera CCD in the experimental setup. In the next epigraph, related with the experimental result, it is necessary to know the system magnification to determine the objects size. The image and the focal planes are related by a Fourier transformation, thus longitudinal distances in the image plane can be extracted by the reciprocal longitudinal distances in the focal plane. In the working conditions with the capture of one hologram, figure 3a, the Fraunhofer pattern is reconstructed, figure 3b. A micrometric scale *Mitutoyo®* with 100 lines per mm was used as object.

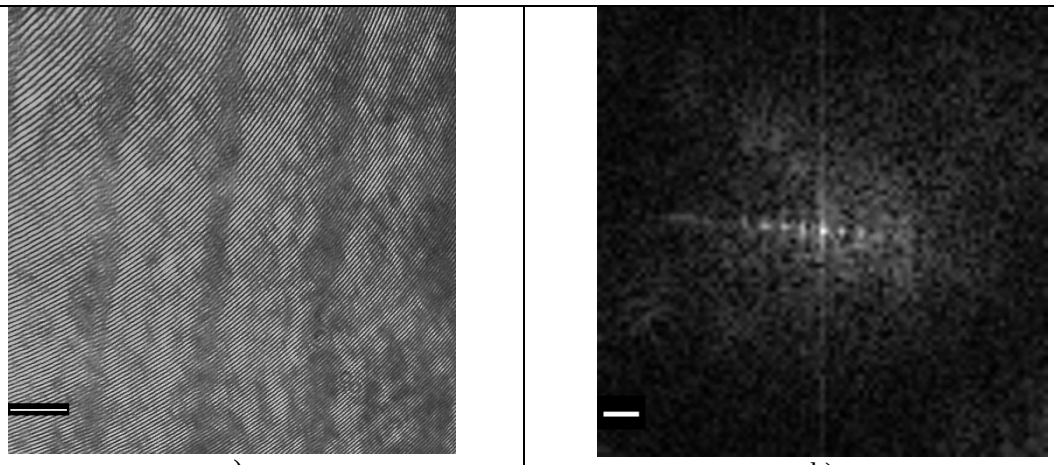

a) b)

Figure 3. a) Calibration scale hologram, scale bar 445 μm, b) Fraunhofer pattern, scale bar 2 $mm^{-1}$

The magnification of the system $M_T = d_i/d_o$ can be determined by the relation of the two equivalent distances $d_i$ and $d_o$ in the image and object plane respectively. We determine the distance $d_i = 0.89$ *mm*

between two bar in the image plane as the reciprocal value of the measured distance $d_f = 1.12$ *mm* between two contiguous spot on the Fraunhofer pattern. With the knowledge that distance $d_o = 10$ *μm*, $M_T = 0.89/0.010 = 89$.

## 5. Experimental results

The Fraunhofer diffraction from multiple apertures is a common occurrence. In this work two different kinds of samples are considered to calculate lineal dimensions in objects with similar forms and two types of spatial distributions, random and periodically distributions.

### *5.1. Random distribution of similar objects*

In the first result we consider a sample of mouse blood cell as an example of random distribution of similar objects and use the proposed methodology to determine the diameter of cells. Figure 4a shows the hologram registered with the experimental setup presented in figure 1.

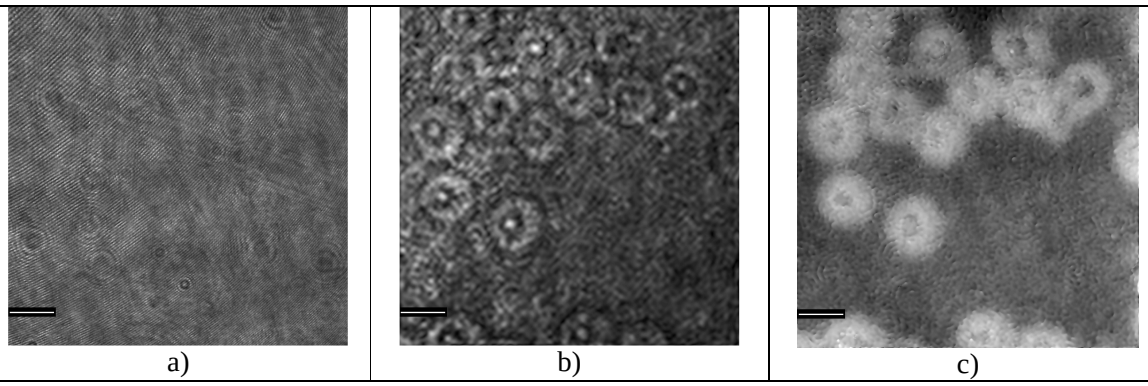

a) b) c)

Figure 4. Image reconstruction. a) Digital hologram, b) Intensity image and c) phase image. Scale bar 5 μm

In figures 4b and 4c are showed the intensity and phase images calculated by equations (4) and (5) respectively. Due to image plane hologram capture, the reconstruction distance was $d' = d_j = 0$. It can be noted that with DPM method the phase image can be reconstructed with the capture of only one hologram. Applying Eq. (2) the Fraunhofer pattern is obtained, figure 5a.

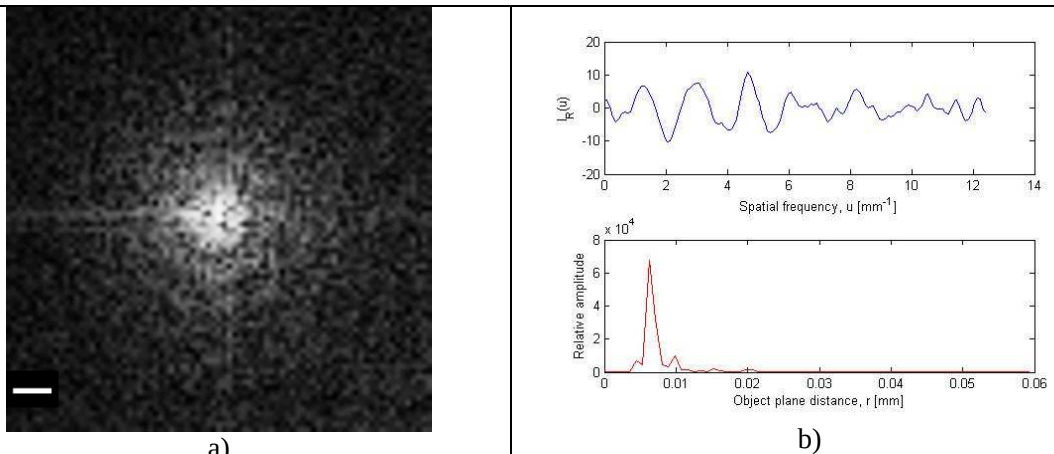


a) b)

Figure 5. a) Fraunhofer pattern, scale bar 2 mm$^{-1}$. b) up- the radial intensity curve $I_R(r)$, down- spectrum of $I_R(r)$

In figure 5a the expression $\left\{1+\log\left[\left|\psi(u,v,d=D)\right|\right]\right\}$ was used to better visualization of intensity distribution of the reconstructed wavefields. As it is predicted by theory, the Fraunhofer diffraction pattern has a 'spotty' interference pattern, with a central peak and intensity in the diffraction plane that shows random fluctuations on a general background.

The radial intensity distribution $I_R(r)$, figure 5b-up, is measured by scanning the Fraunhofer diffraction pattern along radial lines. For each $r$ value the intensity $I_R(r)$ is the result of averaging the intensity values $I_{SFTF}(x', y', z = D)$ along the circumference from $0^o$ to $360^o$, mathematically this operation can be represented by the expression,

$$I_R(r) = r^3 \frac{\sum_{\theta=1}^{360} I\left(x' = C_x(r,\theta), y' = C_y(r,\theta), d' = D\right)}{360} \tag{6}$$

where, $C_x(r,\theta) = \frac{N}{2} + r\cos\theta$, $C_y(r,\theta) = \frac{N}{2} - r\sin\theta$, with $0^o < \theta \leq 360^o$ and $0 < r \leq N/2$.

The spectral analysis of the radial intensity curve $I_R(r)$ is carried out by the calculation of the square of the module of its 1D Fourier transform. In the resulting spectrum, figure 5b-down, the harmonic components are visualized. As seen, only one fundamental harmonic that characterizes the diameter ($r_o = 6.3\ \mu m$) of the mouse blood cell appear.

*5.2. Regularly repeated identical objects*

In the second result we consider a sample of periodically hexagonal structures grabbed on a plastic material with an ions beam as an example of regularly repeated identical objects. In figure 6 is showed the hologram and intensity image reconstruction with the parameters for hexagonal real space lattice.

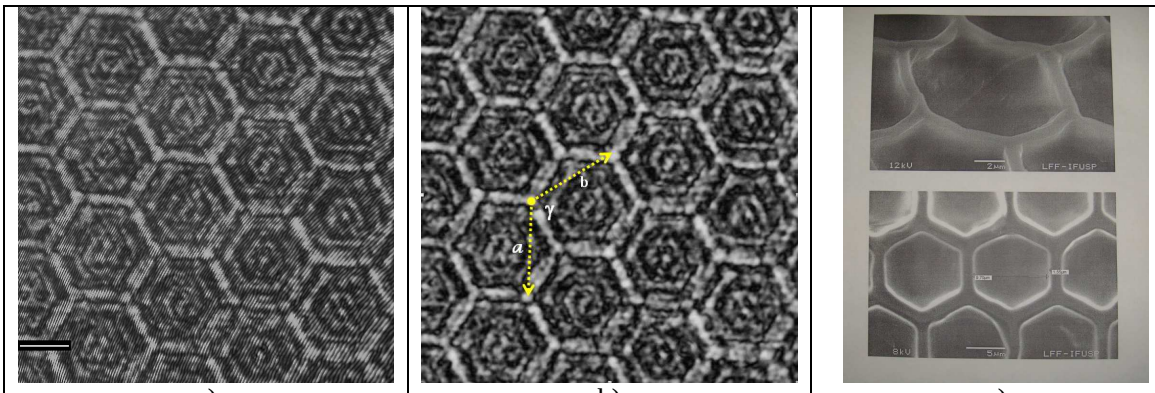


a) b) c)

Figure 6. a) Digital hologram, b) Intensity image. Scale bar 5 μm. c) Image of the object using A*tomic* F*orce* M*icroscopy* (AFM).

In the reconstructed intensity image the parameters for the hexagonal real space lattice on the image plane are showed: diffraction angle for hexagonal crystal $\gamma = 120^o$ and the unit cell parameters $a$, $b$ which for hexagonal crystal met the condition, $a = b$.

Using Eq. (2) the Fraunhofer diffraction pattern is calculated and showed in figure 7a. In figure 7b a section of the reciprocal lattice it is identifying and drawn through the spots, the parameters $a^*$, $b^*$ and $\gamma^*$ are showed in this figure.

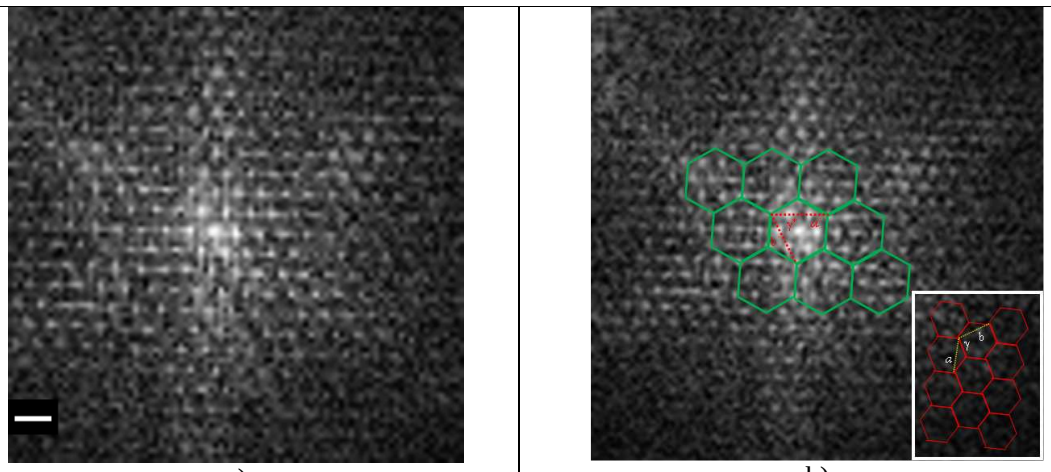

a) b)

Figure 7. a) Fraunhofer diffraction pattern, scale bar 2 $mm^{-1}$. b) Over diffraction pattern it is drawn the reciprocal lattice. (***Inset:*** *Representation of the real space*)

As shown in figure 7b, according to the theory of crystal diffraction [27], the reciprocal lattice edges of dimensions $a^*$ and $b^*$ are respectively perpendicular to the cell edges $b$ and $a$, and quantity are related by the following expressions,

$$a^* = \frac{K}{a \sin \gamma^*},\ b^* = \frac{K}{b \sin \gamma^*} \text{ and } \gamma^* = 180^o - \gamma \tag{7}$$

where $K = \lambda L$ is the constant of diffraction, where $\lambda$ the wavelength of monochromatic radiation and $L$ is the camera length, i.e., the distance from the specimen to the diffraction plane.

Applying the relations (7) the diffraction angle in the reciprocal lattice $\gamma^* = 60^o$ is determined and by measuring the parameters $a^* = b^* = 1.15\ mm$ in the reciprocal lattice it is calculated the parameters $a' = b' = 863\ \mu m$. It can be notice that $a'$ and $b'$ are the real lattice parameters, but in the image plane. The parameters $a$, $b$ of real lattice in the object plane are obtained dividing $a'$ and $b'$ by the total system magnification $M_T = 89$, i.e., $a = b = a'/M_T = b'/M_T = 9.69\ \mu m$. This value coincides with that obtained by AFM, as it is showed in figure 6c.

## 6. Conclusions

In this work it was demonstrated the potentiality of DHM for microscopic objects analysis starting for the calculation of their Fraunhofer diffraction pattern. Using digital hologram reconstruction as a method for calculating the amplitude and intensities distributions of the optical field in the Fourier Transform plane was discussed. The proposed methodology was applied to the mouse blood red as random distribution of similar objects. The spectral analysis of the radial intensity curve on the Fraunhofer diffraction pattern allows the diameters determination of cells. Also, for regularly repeated identical objects distribution the parameters of real lattice was obtained by the identification and measurements of the reciprocal lattice parameters on the Fraunhofer diffraction pattern. With this methodology, all measurements are done automatically, therefore, errors in the determination of the calculated magnitudes is in correspondence with the quality of the optical-electronic components used in the experimental setup. Many applications to the biological and materials sciences can be accomplish with the principles of this research.

**7. Acknowledgements**
This work was supported by the Brazilian agency FAPESP; Process FAPESP No. 2009/50438-7, PV-Prof. Jorge O. Ricardo Perez in July 2009-january 2010.

**8. References**

[1] Palacios D, Palacios F, Viloria T 2006 Quantification and Differentiation of Nuclear Tracks in Nuclear Track Detectors by Simulation of their Diffraction Pattern Applying Fourier Optics *Rev. Mex. Fís.* [0035-001X] **52** 3 214

[2] Palacios F, Ricardo J, Palacios D, Gonçalves E, Valin J, De Souza R 2005 3D image reconstruction of transparent microscopic objects using digital holography *Opt. Commun*.**248** 41

[3] Palacios F, Palacios D, Palacios G, Gonçalves E, Valin J, Sajo-Bohus L, Ricardo J 2008 Methods of Fourier optics in digital holographic microscopy, *Opt. Commun*. **281** 550

[4] Gwo-Huei Y Gwo-Huei Y, Hone-Ene H, and Pin H 2002 Diffraction Limit for a Circular Mask with a Periodic Pinhole Array Jpn. J. Appl. Phys. **41** 2018

[5] Joachim O, Katja S, Karsten K and Michael N 2004 Diffraction by image processing and its application in materials science, Fraunhofer-Institut für Techno- und Wirtschaftsmathematik ITWM ISSN 1434-9973, Bericht 67.

[6] Ananth A, Akwete A 1996 An analysis of the Fraunhofer Diffraction method for particle size distribution analysis and its application to aerosolized sprays *Inter. J. of Pharm*. **127** 219

[7] Zhang C, Lijun X and Jie Ding 2009 Integral inversion to Fraunhofer diffraction for particle sizing *Appl. Opt*. **48** 25 4842

[8] Weber A P, Xu L J and Kasper G 2000 Simultaneous in situ measurement of size, charge and velocity of single aerosol particle *J. Aerosol Sci***. 31** 1015

[9] Greaves D, Boxall J, Mulligan J, Montesi A, Creek J, Dendy-Sloan E and Koh C A 2008 Measuring the particle size of a known distribution using the focused beam reflectance measurement technique *Chem. Eng. Sci*. **63** 5410

[10] Curtis D B, Aycibin M, Young M A, Grassian V H and Kleiber P D 2007 Simultaneous measurement of light-scattering properties and particle size distribution for aerosols: application to ammonium sulfate and quartz aerosol particles *Atmos. Environ.* **41** 4748

[11] Zhao B, Yang Z, Johnston M V, Wang H, Wexler A S, Balthasar M and Kraft M 2003 Measurement and numerical simulation of soot particle size distribution functions in a laminar premixed ethylene-oxygen-argon flame Combust. *Flame* **133** 173

[12] Jagodnicka A K, Stacewicz T, Karasinski G, Posyniak M L and Malinowski S P 2009 Particle size distribution retrieval from multiwavelength lidar signals for droplet aerosol *Appl. Opt.* **48** B8

[13] Hodkinson J R 1966 Particle sizing by means of the forward scattering lobe *Appl. Opt.* **5** 839

[14] Ubera J V, Aguilar J F and Gale D M 2007 Reconstruction of particle-size distributions from light-scattering patterns using three inversion methods *Appl. Opt*. **46** 124

[15] Riefler N and Wriedt T. 2008 Intercomparison of inversion algorithms for particle-sizing using Mie scattering Part. *Syst. Charact.* **25** 216

[16] Streekstra G J, Hoekstra A G, Nijhof E and Heethaar R M 1993 Light scattering by red blood cells in ektacytometry: Fraunhofer versus anomalous diffraction *Appl. Opt.* **32** 13

[17] Seebacher S, Osten W, Baumbach T and Jüptner W 2001 The determination of material parameters of microcomponents using digital holography *Opt. Lasers Eng* **36** 103

[18] Buraga-Lefebre, Coëtmellec S, Lebrun D and Özkul C 2000 Application of wavelet transform to hologram analysis: three-dimensional location particles *Opt. Lasers Eng.* **33** 409

[19] Kreis T and Jüpner W 1997 Principles of digital holography *Akademie Verlag (Series in Optical Metrology*) **3** 353

[20] Grilli S, Ferraro P, De Nicola S, Finizio A, Pierattini V and Meucci R 2001 Whole optical wavefields reconstruction by Digital Holography. *Opt. Express* **9** 294

[21] Palacios F, Palacios D F, Goncalves E, Palacios G, Sajo-Bohus L, Ricardo J, Valin J 2010 *3D* Nuclear Track Analysis By Digital Holographic Microscopy *Radiat. Mea.* doi: 10.1016/j.radmeas.2010.08.011

[22] VanLigten R F and Osterberg H 1966 Holographic Micrsocopy *Nature* **211** 282

[23] Palacios F, Ricardo J, Font O, Palácios G, Palácios D, Gonçalves E, Valin J, Muramatsu M and Lopez M 2010 Digital image reconstruction by double Propagation Method *Opt. Commun.* article in press

[24] Palacios F, Palacios D, Gonçalves E, Palacios G, Valin J, Sajo-Bohus L and Ricardo J 2008 Methods of Fourier optics in digital holographic microscopy, *Opt. Commun*. **281** 550

[25] Cuche E, Marquet P, and Depeursinge C 2000 Spatial filtering for zero-order and twin-image elimination in digital off-axis holography *Appl. Opt.* **39** 4070

[26] Lipson S G, Lipson H 1981 Optical Physics, Second edition. Cambridge University Press

[27] 1999 Image analysis of electron micrographs, SPRING 211